Hindawi
Shock and Vibration
Volume 2019, Article ID 9395354, 13 pages
https://doi.org/10.1155/2019/9395354

Research Article

A Novel Experimental Technique to Simulate Shock Behaviour and Bursting Failure of Roadways

Gui-feng Wang,[1,2] **Si-yuan Gong**,[1] **Lin-ming Dou**,[1] **Geng Li**,[1] **Wu Cai**,[1] **and Chao-jun Fan**[2]

[1]*State Key Laboratory of Coal Resources and Safe Mining, School of Mines, China University of Mining and Technology, Xuzhou 221116, China*
[2]*Department of Energy and Mineral Engineering, G3 Center and Energy Institute, The Pennsylvania State University, University Park, State College, PA 16802, USA*

Correspondence should be addressed to Si-yuan Gong; gsy_cumt@cumt.edu.cn and Lin-ming Dou; lmdou@126.com

Received 17 August 2019; Accepted 19 September 2019; Published 20 November 2019

Academic Editor: Chengzhi Shi

Rockburst is a sudden and dynamic failure of rock that can cause serious injury to miners and damage to the underground excavations. Stress path, dynamic disturbance, and support system play important and different roles in the generation processes of rockbursts, resulting rockbursts with variety of reasons and failure modes. A test facility that was capable of simulating such factors was developed to study shock behaviour and bursting failure of roadways. The results demonstrate that the modeled roadway was in good condition and retained a shock resistance capacity after three drop loads. Until the acceleration amplitude increased to a certain level at the time of the fourth dynamic loading, sudden bursting failure of modeled roadway occurred. Many large fragments ejected from the upper and middle regions of the roadway, accompanied with loud noise. A deep pit was observed after the bursting failure. The axial of the fan-shaped pit had an angle above the vertical. In addition, shock behaviour of the modeled roadway had been changed by the anchor-net support. Significant differences appeared between the acceleration signals measured in two roadway sections with and without the anchor-net support. The acceleration magnitude of the supported roadway section was strongly reduced by the presence of the anchor-net support. Even when the unsupported roadway section underwent a sudden injection failure, the roadway with anchor-net support was in good condition. This study may eventually lead to a methodology for studying the rockbursting resistance capacity of underground roadways.

1. Introduction

Rockburst is a sudden and violent rock failure process occurring with a large energy release, posing a serious threat to the production and safety in underground mining and rock engineering. Many rockbursts, particularly large damaging events, occur spontaneously and unexpectedly. In China, more than 200 coal mines have suffered rockbursts as mining depths increase [1]. On 11 November 2017, a bursting failure of the roadway occurred in the 702 working face in Hongyang No. 3 Coal Mine (Shenyang City, Heilongjiang Province, China), resulting in the closure or semiclosure of a nearly 200 m long section of the roadway [2]. On 20 October 2018, a rockburst in Longyan Coal Mine in Yancheng City caused the closure of 100 m long sections of a tunneling roadway, trapping 22 miners and killing 21 miners in spite of a valiant rescue effort [3]. Rockburst occurrence is closely related to stress path, dynamic disturbance, and support system [4–9]. These factors play important and different roles in the generation processes of rockbursts, resulting rockbursts with a variety of reasons and failure modes. Thus, in spite of many attempts in this research, the rockburst mechanism is still not clear, and effective means of assessing the hazards have not yet been developed because of the difficulty in identifying the influence degrees of stress path, dynamic disturbance, and

support system in underground engineering with complex and diverse geological condition and mining environment.

Rockburst in coal mines represents a failure behaviour of the whole roadway structure, including the support system and coal-rock masses surrounding the roadway [4, 10]. A good understanding of the shock behaviour and failure process of the whole roadway structure is helpful for gaining insight into the rockburst mechanism and designing effective rockburst support system for safety in underground engineering. In recent years, dynamic testing techniques have been used to provide an insight into the dynamic performance and capacity of different underground roadway supports, including the Noranda Technology Center/CANMET Dynamic Testing Apparatus, the Western Australian School of Mines (WASM) Test Facility, Steffen Robertson, Kirsten Consultants (SRK) Drop Weight Test Facility, and a Pendulum Impact Test Facility designed for laboratory testing of modeled roadway under horizontal dynamic loads [11–13]. These facilities mainly focus on the performance testing of reinforcement units and not the whole roadway. They were limited on the ability to test factors such as stress path, dynamic disturbance, and support system that all affect the rockburst occurrence enormously. Because rockbursts occur spontaneously and unexpectedly in situ, it is very difficult to monitor the shock behaviour of the roadway and study the bursting failure process at the excavation scale. Laboratory rockburst experiments play an important role in understanding the rockburst mechanism. Physical model testing on small-scale models can be used to observe the failure of underground roadways. However, laboratory testing of the shock behaviour and bursting failure of modeled roadways under coupled static and dynamic loading remains at an exploratory stage due to the lack of effective methodologies and facilities [12, 13].

Based on the study of the effects of stress path, dynamic disturbance, and support system on the rockburst, a test facility that was capable of applying coupled static and drop weight dynamic loads and simulating factors of stress path, dynamic disturbance, and support system was developed to study shock behaviour and bursting failure of roadways. Acceleration signals of the modeled roadway were recorded in vertical and horizontal directions by an ultradynamic signal monitoring system. A high-speed camera was used to record the real-time failure processes. Differences of the shock behaviour and failure characteristic between roadway sections with and without the anchor-net support were investigated. Relevant studies remain both rare and limited. This study may eventually lead to a methodology for studying the rockbursting resistance capacity of underground roadways, which would provide a significant advance in the research into the rockburst mechanism.

2. Influencing Factors of a Rockburst

2.1. Static Stress. A rockburst is caused by the abrupt release of elastic energy stored in coal-rock masses. Therefore, an accumulation of sufficient energy is the premise for the occurrence of rockbursts. The energy accumulation is induced by stress concentration. Static stress in underground engineering is generated by the combination of geo-stress and mining-induced stress [14, 15]. Geo-stress is an important factor for the occurrence of rockbursts in underground excavations. It has been observed for a long time that both the severity of rockbursts and their frequency increase with the depth of underground engineering. Increasing weight of the overburden and therefore increasing stresses in the coal-rock masses with depth are the cause [16]. That is with the increasing depth of underground engineering, the ability of coal-rock masses to store significant amounts of energy increases. Research findings reveal that the higher the strain energy that can be stored in coal-rock masses, the higher its tendency to burst [4, 15]. It has been observed in many coal mines that rockbursts start at a depth of 600–800 m [17–19]. As shown in Figure 1, Table 1, and Figure 2, rockbursts frequently occurred both in coal seams 11 and 17 of Xing'an Coal Mine when the mining depths approached 600 m in the two coal seams, while there were no rockbursts before this depth.

Faults and folds are common in strata. Many rockbursts are the consequence of the combined effect of mining activities and local tectonic stress. For example, the 250204 working face of Yanbei Coal Mine located in the region with a syncline structure. Fifty rockbursts happened in 250204 working face from April 2011 to May 2013 in Yanbei Coal Mine [7]. As shown in Figure 3, the time interval increased while the released energy rapidly reduced as the working face advanced away from the axis of the syncline, indicating that the rockburst danger gradually decreased. This phenomenon provides evidence that the geo-stress exerts a significant effect on the occurrence of rockbursts. Meanwhile, additional stress induced by mining operations can superimpose with the geo-stress, generating further stress concentration.

2.2. Dynamic Disturbance. Researchers and mining engineers have gradually reached a consensus, whereby static stress and dynamic disturbance both play important roles in the occurrence of rockbursts [4, 21]. A rockburst may occur when the total stress (due to the superposition of static stress and dynamic disturbance) within the coal-rock masses reaches a certain critical level [18, 22]. In this regard, rockbursts are likely to occur when the rock mass is firstly under the high static stress induced by the geo-stress and excavation and is secondly triggered by a dynamic disturbance. A sudden failure of a loaded structural unit of rock mass will induce a tremor which provokes seismic waves propagating through rock mass, providing additional stress (dynamic stress) in the surroundings of roadways [21, 23]. Numerous and low-energy tremors often occur before strong tremors. However, only few strong tremors were manifested as rockbursts in roadways [7, 10]. This phenomenon indicated that the occurrence of rockbursts requires adequate dynamic disturbance to trigger the abrupt release of energy stored in coal-rock masses. When the total stress nearby the roadway reaches a certain critical level with the superposition of static and dynamic stresses, a rockburst with abrupt release of energy stored in coal-rock masses is prone to occur.

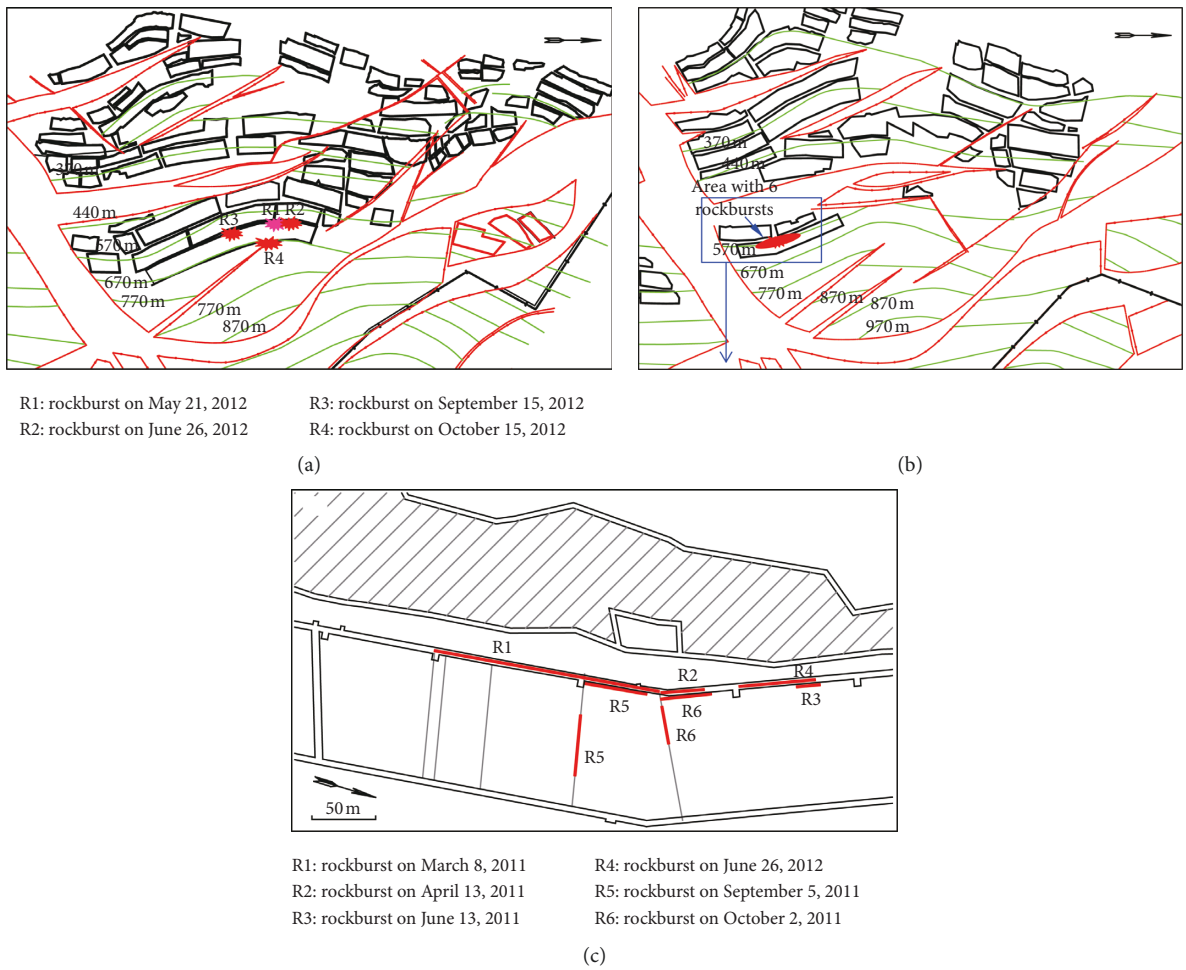

Figure 1: Rockbursts in coal seams 11 (a), 17 (b), and 17's local magnification (c) when the mining depths of Xing'an Coal Mine approached 600 m.

Table 1: Further details related to the consequences of rockbursts.

Coal seam no.	Date	Damage range of roadways (m)	Depth of roadway (m)	Description of rockburst damage
17	2011.3.8	180	≥570	A 40 m long section of roadway was almost closed with floor heave 2.2–2.4 m, and convergence of two side walls was 3.2–3.4 m
17	2011.4.13	36	≥570	Maximum convergence of side walls was 1.0–1.8 m, and maximum floor heave was 1.0–1.3 m. The tunnel machine was overturned
17	2011.6.13	10	≥570	The tunnel machines were bounced and shifted to the lower side wall
17	2011.6.26	60	≥570	Floor heave in roadway was 0.8 m
17	2011.9.5	50	≥570	Severe local ejection occurred in coalfaces. Floor heave in roadway was 0.5–1.0 m
17	2011.10.2	40	≥570	Roadway converged to 1–1.5 m
11	2012.5.21	70	≥570	Convergence of two side walls is 1.5–2.0 m. A 20 m long section of the roadway was almost closed
11	2012.6.26	45	≥570	The height of roadway was changed to 0.6–0.8 m, and the width was reduced to about 1 m
11	2012.9.15	35	≥570	A 35 m long section of roadway being excavated was seriously damaged. Convergence of two side walls was 0.5–1.7 m
11	2012.10.15	104	≥670	Convergence of two side walls was 0.5–1.0 m. Roof subsidence was 0.5–1.0 m

Figure 2: Photos of rockburst damage in Xing'an Coal Mine, roof subsidence and floor heave (a), coalface damage (b), convergence of two side walls (c), and damage of U-type steel (d).

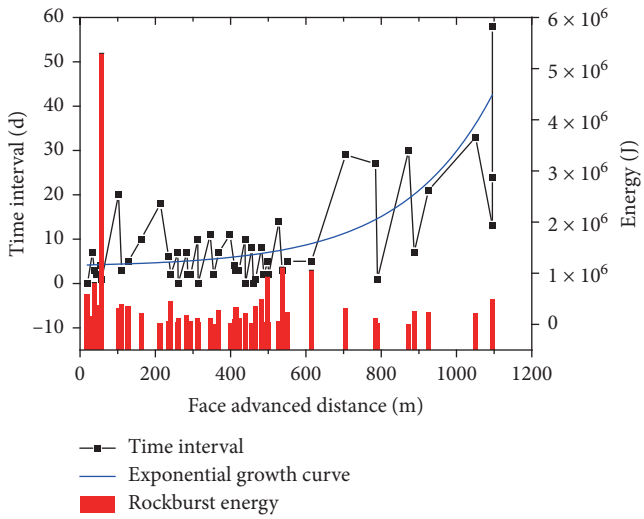

Figure 3: Time interval and the energy of rockbursts regarding the advanced distance of the coalface in Yanbei Coal Mine [7].

2.3. Support System. Rockburst occurrence is also closely related to the shock resistance capacity of the roadway. Once failure is triggered, the severity of the damage depends on the energy that is released during the failure process and the support system. The volume of released energy depends on the extent of the excessively stressed zone and intensity of stress concentration nearby the roadway. Meanwhile, it has been observed in many coal mines that optimum support measures can prevent or at least reduce rockburst effects. It is regarded that effective support system can hold and retain the broken rock, but, more importantly, it can control and minimize the bulking process. Thus, effective support can reinforce the rock mass, promote the shock resistance of a roadway, and reduce or prevent the damage of rockbursts [24–26].

3. Experimental Methods

3.1. Drop Hammer Impact Test Facility. A drop hammer impact test facility was designed for laboratory testing of shock resistance of the roadway under dynamic loading. The facility is capable of producing the dynamic stress wave and providing flexibilities for investigators to design different static and dynamic stress combinations. Figures 4(a) and 4(b) show the schematic diagram and an overview of the facility. The facility consists of a gate-shaped steel frame, hydraulic loading device, and drop hammer impact system. The hydraulic loading device can provide loads in vertical and horizontal directions, respectively. Dynamic

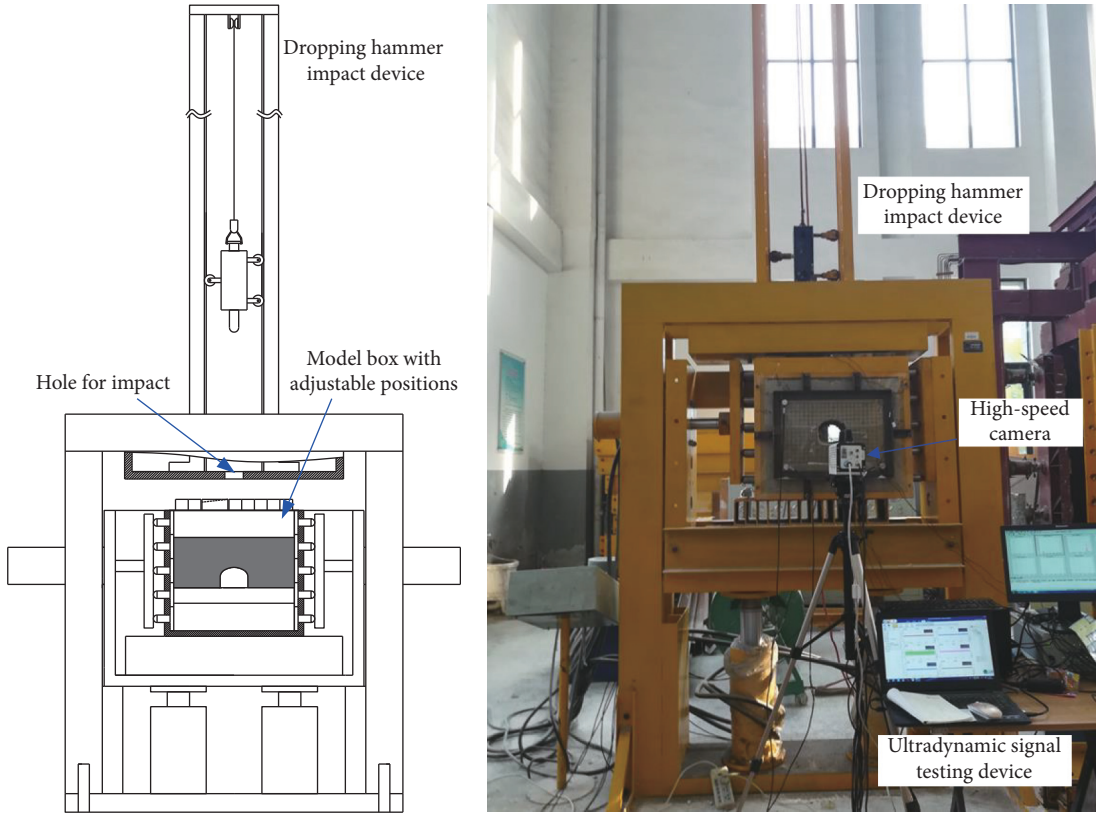

Figure 4: Schematic diagram (a) and an overview of the drop hammer impact test facility (b).

loads were produced by the sudden drop of a hammer to cause a sudden impact on a plate that was placed on the top of the model and had a slant face (9° above the horizontal). The facility can simulate the energy release at different levels by simply controlling the drop height of the 20 kg hammer. The main advantages of this facility are that the setup is relatively inexpensive, the configuration provides consistent and repeatable tests, and the facility could undertake multiple tests on the same roadway model. In addition, the drop hammer impact test facility is well instrumented as it can measure acceleration, displacements, and the bursting failure process of the modeled roadway. The facility had a maximum drop height of 2.6 m that would imply a potential velocity of 7.14 m/s, with a kinetic energy of 509.6 J.

3.2. Model Building and Test Procedures. The physical model represented the geological conditions around a roadway in Xing'an Coal Mine, Hegang City (Heilongjiang Province, China). Physical and mechanical properties of the natural and model rocks are displayed in Table 2. The model dimensions (width × height × thickness) are 700 mm × 650 mm × 400 mm, as shown in Figure 5. To simulate an arched underground cavern with a bottom width of 4.0 m and a centerline height of 3.0 m, the geometric scale factor C_l, defined as the ratio of the dimension of the real rock mass to the roadway model, was determined to be 26.7. Thus, the modeled roadway was excavated with a bottom width of 150 mm and a centerline height of 112.5 mm. Calculated with $C_\sigma = C_l \times C_\rho$ and $C_E = C_\rho \times C_l^4$ according to similarity theory [20, 27, 28], the similarity ratios of density, force, and energy were $C_\rho = 1.37$, $C_\sigma = 36.43$, and $C_E = 6.96 \times 10^5$, respectively. Based on the force scale factor, stresses of 0.82 MPa and 0.6 MPa were applied to the model in the horizontal and vertical directions, respectively, to simulate the in situ vertical stress of 30 MPa and horizontal stress of 22 MPa. Thus, the experimental data can possibly be correlated to in situ conditions and become usable for design purposes.

The test procedures are as follows: (1) the roadway model was gradually loaded until stresses in vertical and horizontal directions reached the predefined initial stress state; (2) the modeled roadway was excavated; and (3) the hammer was raised to the height of 200 mm. If bursting failure did not occur, then the drop height of the hammer was varied in increments of 200 mm. The modeled roadways were impacted four times with corresponding energy (39.2 J, 78.4 J, 117.6 J, and 156.8 J), until bursting failure of the modeled roadway occurred. The tremor energy measured in coal mines was basically 0.26–3.6% of the total energy released in coal-rock masses [29]. Based on the similarity ratio of energy and the results of surveys on the absorption efficiency of the dynamic energy generated in similar tests [13, 22, 30], the

Table 2: Mechanical and material properties of rocks.

Natural rock properties				Model materials and ratios		Modeled rock properties		
Lithology	Unit weight (kN/m^3)	Compressive strength (MPa)	Young's modulus (GPa)	Ratio of sand and binder	Ratio of cement and gypsum	Unit weight (kN/m^3)	Compressive strength (MPa)	Young's modulus (GPa)
Fine sandstone	24.8	59.75	26.51	6 : 1	5 : 5	18.49	1.782	0.41
Coal seam	13.2	17.92	9.80	8 : 1	5 : 5	17.53	0.821	0.29
Medium sandstone	24.5	71.28	29.88	6 : 1	7 : 3	17.99	1.997	0.40
Coarse sandstone	25.2	81.67	31.39	5 : 1	7 : 3	18.59	2.398	0.44

simulated maximum tremor energy was calculated to be 6.96×10^5 J to 3.34×10^6 J that was equivalent to the energy magnitude of recorded strong tremors.

The model building procedure is shown in Figure 5. As mentioned above, an ultradynamic signal testing system (DH5960) with an acquisition rate of 200 kHz was employed to measure acceleration signals of the modeled roadway under dynamic loading. The impact plate containing two accelerometers (maximum range 30 km/s^2 and frequency band 1 to 20 kHz) in vertical and horizontal directions was located on the top of the roadway model (Figure 5(e)). Four accelerometers were installed in the modeled roadways (Figure 5(f)). These accelerometers were used to measure the acceleration of the impact plate and the acceleration of roadways. After each impact loading, permanent deformations of roadways were measured manually. A high-speed camera (NAC Memrecam GX-3) was placed in front of the physical model and employed to record the abrupt failure process of the roadway structure. The recording speed of the high-speed camera was 1000 frame per second at a resolution of 1024×1024.

The behaviour and failure of the roadway under different dynamic loads were then investigated. The modeled roadway was anchored with aluminum rods with the dimension of $\Phi 2.0\,\text{mm} \times 75\,\text{mm}$ and an interval of $30\,\text{mm} \times 30\,\text{mm}$ (simulating a real interval of $800\,\text{mm} \times 800\,\text{mm}$), according to the equivalent rigidity and the results of surveys on mechanical parameters of a number of materials and model tests [28, 31]. In order to test roadway sections with different support patterns under the same circumstances and dynamic disturbance, the back half (200 to 400 mm) of the modeled roadway was supported with the anchor-net, while the front half (0 to 200 mm) had no support. In this way, shock resistance abilities of roadway sections with and without the anchor-net support were compared under the same experimental conditions.

4. Results and Discussion

As mentioned above, the front half (0 to 200 mm) and back half (200 to 400 mm) of the modeled roadway had no support and anchor-net support, respectively. Accelerations of roadway sections were recorded under different dynamic loads. Acceleration signals from the impact plate and the two roadway sections at different dynamic loading stages are demonstrated in Figures 6 and 7 depicts the changes in acceleration peak of roadway sections with and without the support under dynamic loads. When the lifting height of the drop hammer was increased, the vertical and horizontal acceleration amplitudes monitored by using two accelerometers on the impact plate gradually increased. Meanwhile, acceleration amplitudes of the two roadway sections also increased in vertical and horizontal directions. Significant differences appeared between acceleration signals measured in the two roadway sections with and without anchor-net support. This phenomenon showed that the anchor-net support could change the shock behaviour of the roadway under dynamic loads. That is, the acceleration amplitude of the roadway section without the support increased obviously with the increase of dynamic loading energy, while the acceleration amplitude of the roadway section with the anchor-net support had no obvious increase, especially in the horizontal direction. Under the first three dynamic loads, no failure occurred as the amplitude of shock acceleration of the modeled roadway increased. However, when acceleration amplitude increased to a certain level at the time of the fourth dynamic loading, the unsupported roadway section underwent a sudden failure process, whereas the roadway with anchor-net support displayed no failure. Both the vertical and horizontal acceleration peaks of the unsupported roadway section were higher under the fourth dynamic loading, manifesting the dynamic nature of the bursting failure event. However, the roadway section with the anchor support still had small acceleration peaks at that time. This meant that the shock resistance of the roadway was increased by the anchor-net support.

After three dynamic loads, sudden bursting failure of the modeled roadway occurred at the moment of the fourth dynamic loading (with loading energy of 156.8 J). Figure 8 shows the photographs of the modeled roadway before and after the bursting failure. It was found that after three drop impacts, the modeled roadway was still in good condition without displaying obvious dislocation. Only small particles drop to the floor in the unsupported roadway section

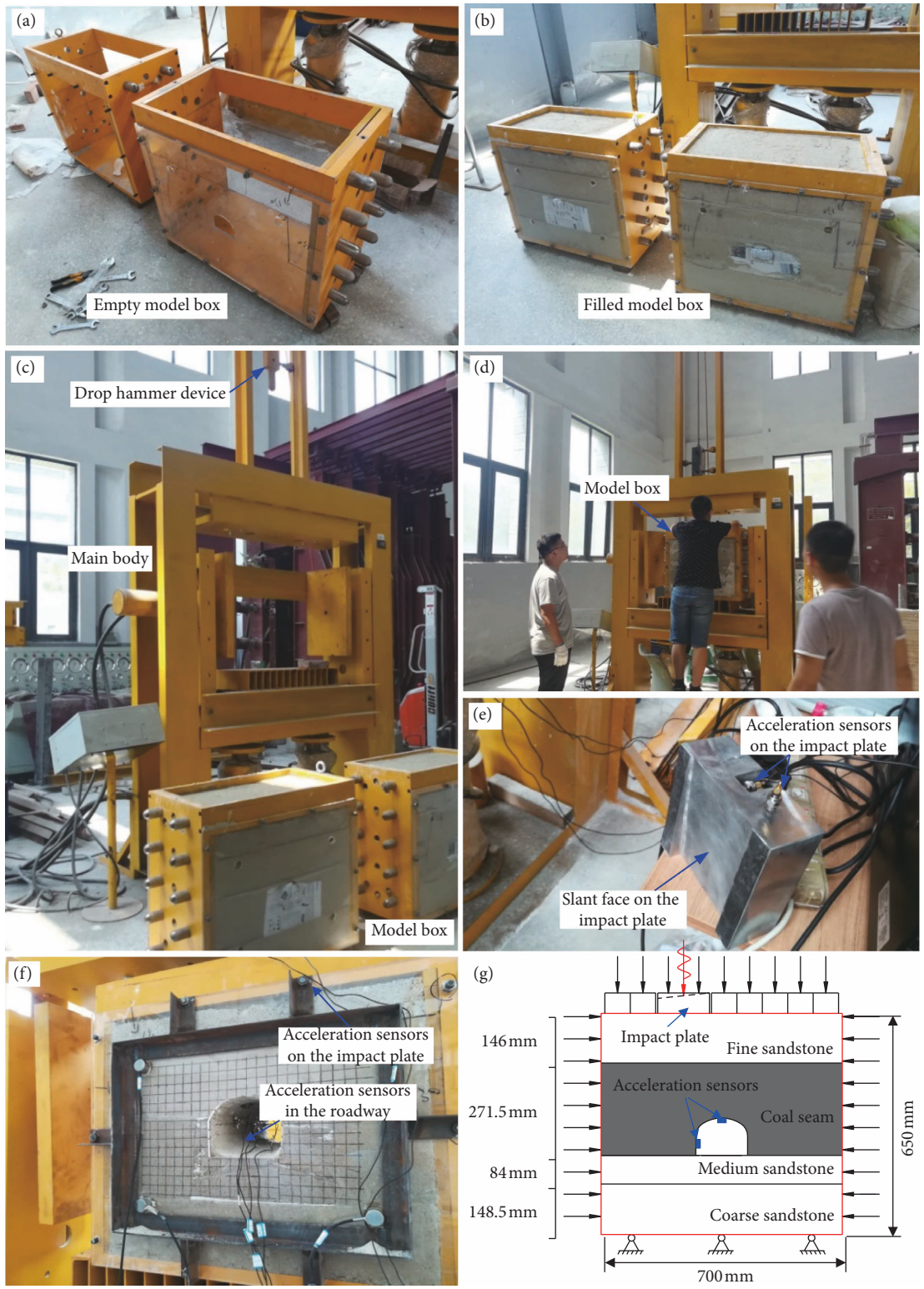

Figure 5: Model building procedure: (a) removing the empty model box from the facility, (b) filling the model box with model materials, (c) air-drying the model, (d) returning the model box to the facility, (e) putting the impact on top of the model, (f) installing sensors and applying loads, and (g) the schematic diagram of the test procedure.

(Figure 8(b)), indicating the modeled roadway retained its shock resistance to dynamic loads at that time. At the time of the fourth dynamic loading with an energy of 156.8 J, bursting failure of the modeled roadway was observed. Figure 8(c) shows that bursting failure of the roadway took the form of a sudden injection with large fragments that part

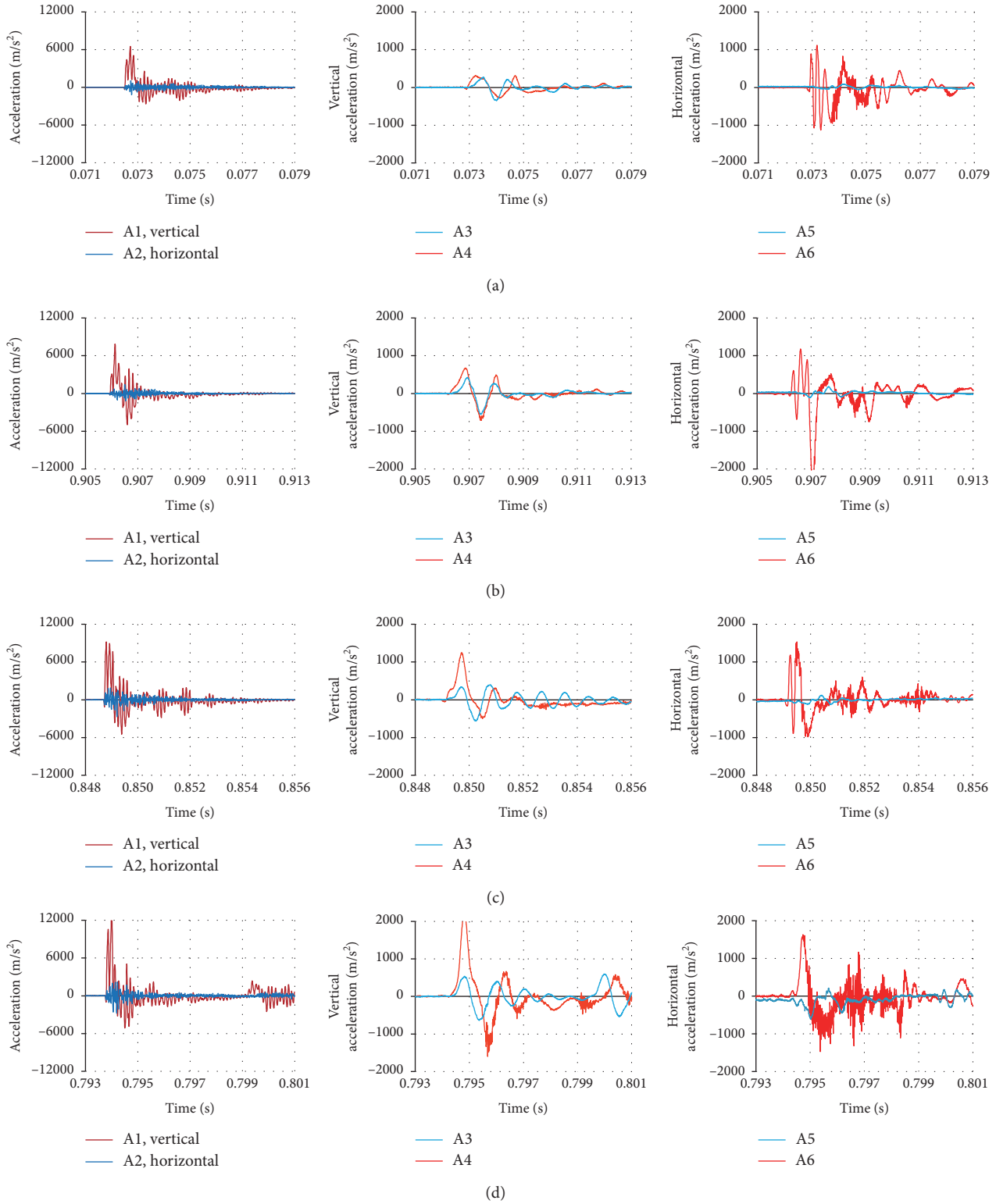

A1, A2: Accelerometers located on the impact plate
A3, A4: Vertical accelerometers in roadway sections with and without the anchor-net support
A5, A6: Horizontal accelerometers in roadway sections with and without the anchor-net support

Figure 6: Acceleration signals in tests with different dynamic loading energy: (a) 39.2 J; (b) 78.4 J; (c) 117.6 J; (d) 156.8 J.

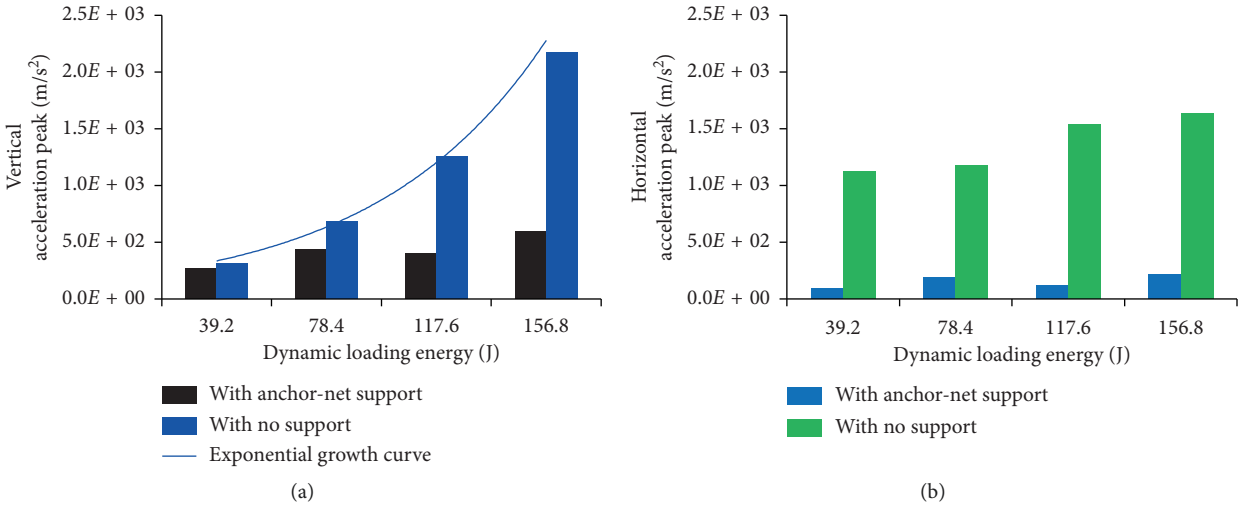

Figure 7: Variations of acceleration peaks in vertical (a) and horizontal (b) directions at different dynamic loading stages.

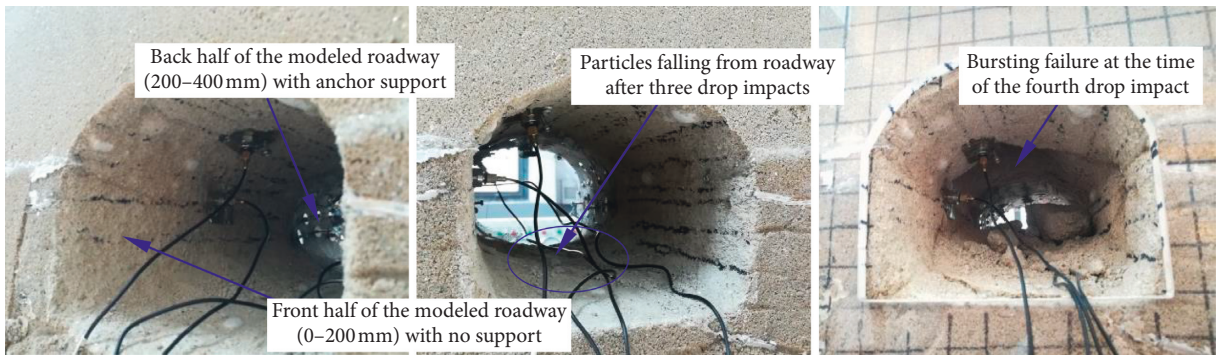

Figure 8: Photographs of the modeled roadway before drop impacts (a), after three drop impacts (b), and after the fourth drop impact (c).

filled the roadway. When the bursting failure occurred, many large fragments ejected from the upper and middle regions, accompanied with loud noise. After the roadway destruction, it was found that the bursting failure occurred in the unsupported roadway section, while the other section with the anchor-net support remained intact. A deep pit damage zone was observed after the bursting failure. This zone was the deepest in the roof.

Rockburst represents a sudden failure behaviour of the whole roadway structure. The damage includes the surrounding rock and the support units. A GX-3 high-speed camera was used to capture the failure process of the modeled roadway. A few images captured from the video are presented in Figure 9. It is a sudden failure with no pre-announcement and pre-event dilatation before the resistance of the roadway was exceeded. During this ejection process, a large piece of fragments jetted out at a high speed with a crisp and loud sound. Figure 10 shows the surface scene after bursting failure. It can be observed that a deep pit was formed after the fragment ejection. Because dynamic stress waves had been generated both in vertical and horizontal directions by using the impact plate with a slant face, the axial of the fan-shaped pit had an angle above the vertical (Figure 10(d)). In the tests, bursting failure only occurred in the unsupported roadway section. However, the roadway section with the anchor-net support was still in good condition. It can be concluded that the back roadway section with anchor-net support had higher shock resistance to dynamic loads. Hence, the resistance of the support is decisive for the occurrence of rockbursts in underground roadways (in view of different shock behaviour and bursting failure of roadway sections with and without the anchor-net support systems).

These laboratory testing results are in line with conclusions of many other studies [13, 18, 24, 32–35]: (1) The occurrence of many rockbursts requires adequate dynamic disturbance induced by tremors to trigger the abrupt release of energy stored in coal-rock masses. It means if a dynamic disturbance can trigger the abrupt release of elastic energy stored in coal-rock masses, a rockburst will occur. Roadway structures under different stress path, dynamic disturbance, and support system can sustain dynamic disturbance of different magnitudes. (2) The acceleration magnitude of the supported roadway section was strongly reduced by the presence of the anchor-net support. This means the anchor-net support system which had the roles such as reinforcement

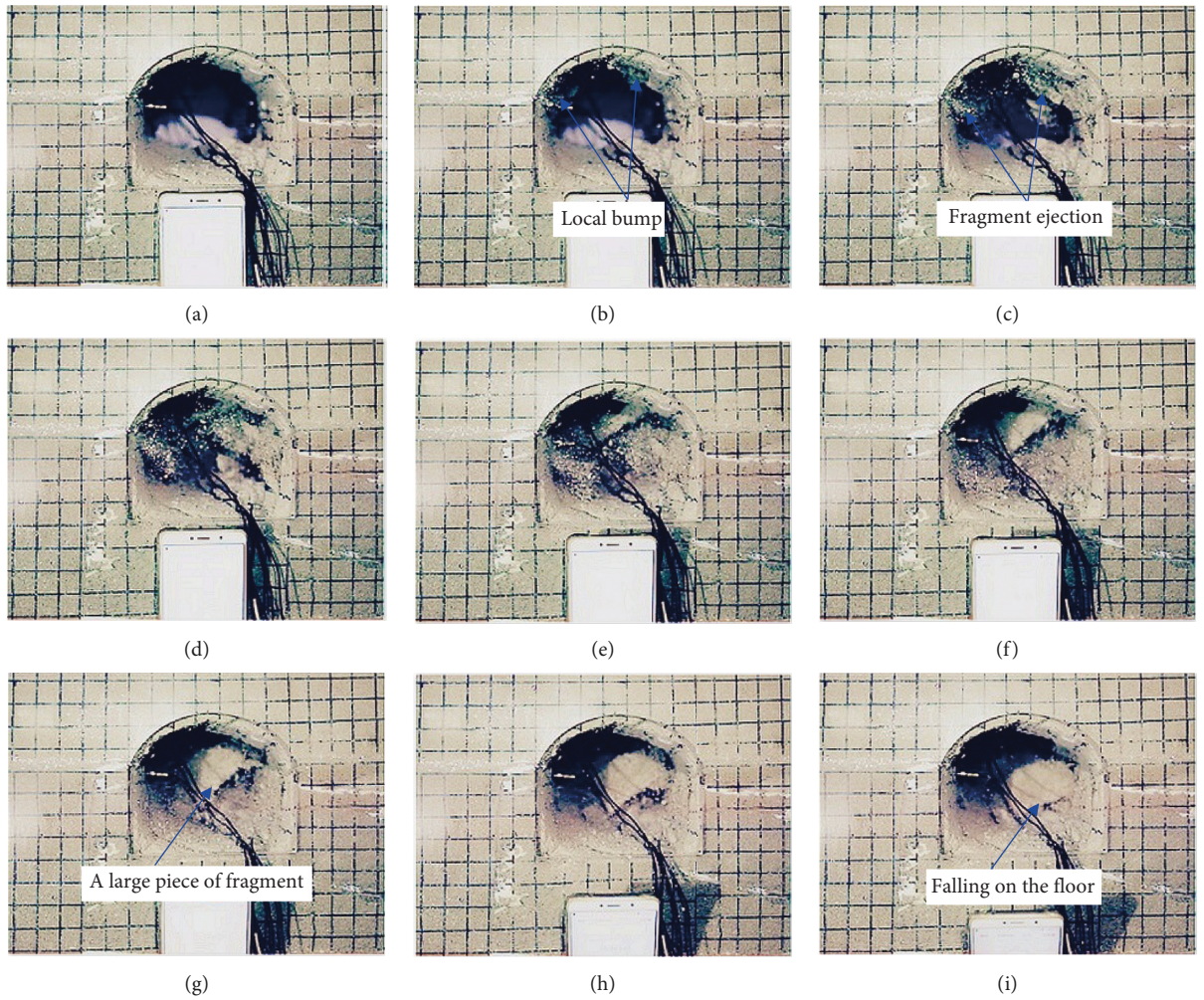

Figure 9: Bursting failure patterns of the modeled roadway recorded with the high-speed camera. (a) 0 ms, (b) 22 ms, (c) 44 ms, (d) 66 ms, (e) 88 ms, (f) 110 ms, (g) 132 ms, (h) 154 ms, and (i) 176 ms.

Figure 10: Continued.

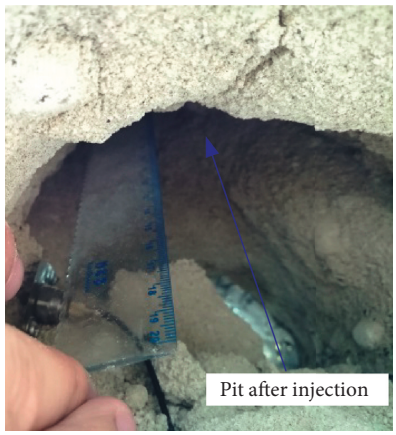

(c)

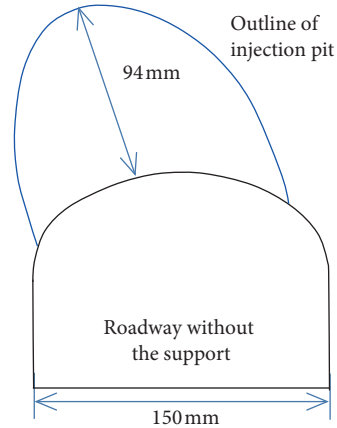

(d)

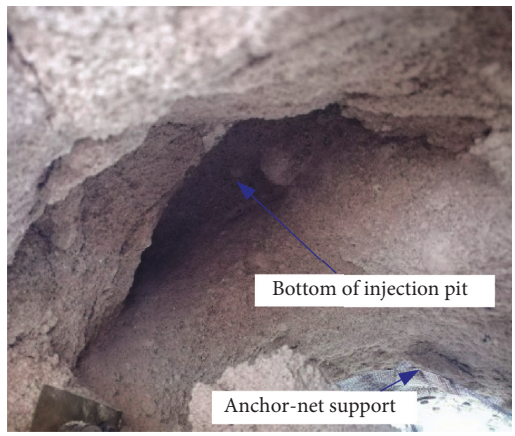

(e)

Figure 10: Surface scenes after bursting failure: (a) roadway section with no support, (b) roadway section with the anchor-net support, (c) large pit after the injection, (d) outline of the injection pit, and (e) bottom of the injection pit.

of rocks, holding, and retaining fractured rocks resulted in substantial improvement in shock resistance of the roadway, thus reducing the incidence of rockbursts in underground roadways. (3) The usage of the retaining mesh that provided good area coverage and a high ductile support also helped anchor-net supported roadway prevent the rock mass to fall down that had occurred in the unsupported roadway section. Hoek et al. [36] defined this function as the strengthening of a jointed rock mass by reinforcement to form a rock arch capable of carrying the induced stresses and helping the rock to support itself. Shah and Hoek [32] stated that the strength of a jointed or fractured mass increases significantly if a skin of broken rock that is held in place generates combing pressure. In addition, the skin also acts to distribute load, thus helping to protect from impact forces. It has not been verified yet but might be possible that the fractured rock acts as a damper, dissipating some of the incoming seismic energy [14].

5. Conclusion

The research provides a novel experimental technique to study shock behaviour and bursting failure of roadways based on the drop hammer impact test facility. The artificially produced rockburst in laboratory tests provides opportunities to observe the rockburst process, which is extremely difficult to be studied in underground engineering. The following conclusions could be obtained:

(1) Adequate dynamic disturbance is needed to trigger the abrupt release of energy stored in coal-rock masses. The modeled roadway was in good condition and retained a shock resistance capacity after three drop loads. Until acceleration amplitude increased to a certain level at the time of the fourth dynamic loading, sudden bursting failure occurred. A fan-shaped pit with an angle above the vertical direction was formed after the fragment ejection.

(2) The resistance of the support is decisive for the occurrence of rockbursts. Anchor-net support changed the shock behaviour of the roadway under dynamic loading obviously. The acceleration magnitude of the supported roadway section was strongly reduced by the presence of the anchor-net support. When the unsupported roadway section underwent a sudden failure process, the roadway with anchored support retained its structural integrity.

Data Availability

The calculation data used to support the findings of this study are available from the corresponding author upon request.

Conflicts of Interest

The authors declare that they have no conflicts of interest.

Acknowledgments

This work was supported by the Fundamental Research Funds for the Central Universities (Grant no. 2017QNA27); Academic Programme for Development of Jiangsu Higher Education Institutions in China (Grant no. SZBF2011-6-B35); State Key Laboratory of Coal Resources and Safe Mining, CUMT (Grant nos. SKLCRSM16X05 and SKLCRSM16X07); National Natural Science Foundation of China (Grant nos. 51504248, 51874292 and 51604270); and State Key Research Development Programme of China (Grant no. 2016YFC0801403).

References

[1] Coal News of China, "How to suppress invisible killers and reduce threats for coal mine safety," 2019, http://xwzx.cumt.edu.cn/27/2e/c522a534318/page.htm.

[2] Bureau of Liaoning Coal Mine Safety Supervision, *Investigation Report on "11.11" Major Roof Accident in Hongyang No.3 Coal Mine*, Shenyang Coking Coal Co., Ltd., Shenyang, China, 2018, http://www.lnmj.gov.cn/zwgk/sgdcbgcx/201809/t20180904_3305829.html.

[3] Bureau of Shandong Coal Mine Safety Supervision, "Press conference on the latest development of relief work held by the emergency relief headquarters of Longyan Coal Industry," 2019, http://www.sdcoal.gov.cn/articles/ch00017/201904/dd5792b8-dbee-414c-b9a2-4fe21da4bd11.shtml.

[4] W. D. Ortlepp, "The behaviour of tunnels at great depth under large static and dynamic pressures," *Tunnelling and Underground Space Technology*, vol. 16, no. 1, pp. 41–48, 2001.

[5] A. Modiriasari, A. Bobet, and L. J. Pyrak-Nolte, "Active seismic monitoring of crack initiation, propagation, and coalescence in rock," *Rock Mechanics and Rock Engineering*, vol. 50, no. 9, pp. 2311–2325, 2017.

[6] H.-W. Wang, Y.-D. Jiang, S. Xue, X.-F. Pang, Z.-N. Lin, and D.-X. Deng, "Investigation of intrinsic and external factors contributing to the occurrence of coal bumps in the mining area of Western Beijing, China," *Rock Mechanics and Rock Engineering*, vol. 50, no. 4, pp. 1033–1047, 2017.

[7] G.-F. Wang, S.-Y. Gong, L.-M. Dou, H. Wang, and A.-Y. Cao, "Rockburst characteristics in syncline regions and microseismic precursors based on energy density clouds," *Tunnelling and Underground Space Technology*, vol. 81, pp. 83–93, 2018.

[8] P. Wang, L.-S. Jiang, P.-Q. Zheng, G.-P. Qin, and C. Zhang, "Inducing mode analysis of rock burst in fault-affected zone with a hard-thick stratum occurrence," *Environmental Earth Sciences*, vol. 78, no. 15, 2019.

[9] W.-B. Sun, H.-Q. Du, F. Zhou, and J.-L. Shao, "Experimental study of crack propagation of rock-like specimens containing conjugate fractures," *Geomechanics and Engineering*, vol. 17, no. 4, pp. 323–331, 2019.

[10] Z.-L. Li, X.-Q. He, L.-M. Dou, and D.-Z. Song, "Comparison of rockburst occurrence during extraction of thick coal seams using top-coal caving versus slicing mining methods," *Canadian Geotechnical Journal*, vol. 55, no. 10, pp. 1433–1450, 2018.

[11] A.-G. Thompson, E. Villaescusa, and C.-R. Windsor, "Ground support terminology and classification: an update," *Geotechnical and Geological Engineering*, vol. 30, no. 3, pp. 553–580, 2012.

[12] J. Hadjigeorgiou and Y. Potvin, "A critical assessment of dynamic rock reinforcement and support testing facilities," *Rock Mechanics and Rock Engineering*, vol. 44, no. 5, pp. 565–578, 2011.

[13] G.-F. Wang, S.-Y. Gong, L.-M. Dou, W. Cai, F. Jin, and C.-J. Fan, "Behaviour and bursting failure of roadways based on a pendulum impact test facility," *Tunnelling and Underground Space Technology*, vol. 92, Article ID 103042, 2019.

[14] Z.-L. Li, X.-Q. He, L.-M. Dou, and G.-F. Wang, "Rockburst occurrences and microseismicity in a longwall panel experiencing frequent rockbursts," *Geosciences Journal*, vol. 22, no. 4, pp. 623–639, 2018.

[15] C.-J. Fan, D. Elsworth, S. Li et al., "Modelling and optimization of enhanced coalbed methane recovery using CO_2/N_2 mixtures," *Fuel*, vol. 253, pp. 1114–1129, 2019.

[16] R. Patynska, "The consequences of the rock burst hazard in the Silesian companies in Poland," *Acta Geodynamica et Geomaterialia*, vol. 10, no. 2, pp. 227–235, 2013.

[17] W. Cai, L. Dou, M. Zhang, W. Cao, J.-Q. Shi, and L. Feng, "A fuzzy comprehensive evaluation methodology for rock burst forecasting using microseismic monitoring," *Tunnelling and Underground Space Technology*, vol. 80, pp. 232–245, 2018.

[18] L.-M. Dou, Z.-L. Mu, Z.-L. Li, A.-Y. Cao, and S.-Y. Gong, "Research progress of monitoring, forecasting, and prevention of rockburst in underground coal mining in China," *International Journal of Coal Science & Technology*, vol. 1, no. 3, pp. 278–288, 2014.

[19] Z.-L. Li, X.-Q. He, L.-M. Dou, D.-Z. Song, and G.-F. Wang, "Numerical investigation of load shedding and rockburst reduction effects of top-coal caving mining in thick coal seams," *International Journal of Rock Mechanics and Mining Sciences*, vol. 110, pp. 266–278, 2018.

[20] P. Wang, L. Jiang, X. Li, G. Qin, and E. Wang, "Physical simulation of mining effect caused by a fault tectonic," *Arabian Journal of Geosciences*, vol. 11, no. 23, p. 741, 2018.

[21] C. Zhang, I. Canbulat, B. Hebblewhite, and C. R. Ward, "Assessing coal burst phenomena in mining and insights into directions for future research," *International Journal of Coal Geology*, vol. 179, pp. 28–44, 2017.

[22] W. Cai, *Fault rockburst induced by static and dynamic loads superposition and its monitoring and warning*, Ph.D. thesis, China University of Mining and Technology, Xuzhou, China, 2015.

[23] J. He, L.-M. Dou, S.-Y. Gong, J. Li, and Z. Ma, "Rock burst assessment and prediction by dynamic and static stress analysis based on micro-seismic monitoring," *International Journal of Rock Mechanics and Mining Sciences*, vol. 93, pp. 46–53, 2017.

[24] P. -K. Kaiser and M. Cai, "Design of rock support system under rockburst condition," *Journal of Rock Mechanics and Geotechnical Engineering*, vol. 4, no. 3, pp. 215–227, 2012.

[25] T.-A. Stacey, "Philosophical view on the testing of rock support for rockburst conditions," *Journal of South African Institute of Mining and Metallurgy*, vol. 112, no. 8, pp. 1–8, 2012.

[26] S. Prusek and W. Masny, "Analysis of damage to underground workings and their supports caused by dynamic phenomena," *Journal of Mining Science*, vol. 51, no. 1, pp. 63–72, 2015.

[27] M.-A. Meguid, O. Saada, M.-A. Nunes, and J. Mattar, "Physical modeling of tunnels in soft ground: a review," *Tunnelling and Underground Space Technology*, vol. 23, no. 2, pp. 185–198, 2008.

[28] W.-S. Zhu, Q.-B. Zhang, H.-H. Zhu et al., "Large-scale geomechanical model testing of an underground cavern group in a true three-dimensional (3-D) stress state," *Canadian Geotechnical Journal*, vol. 47, no. 9, pp. 935–946, 2010.

[29] J. He, L.-M. Dou, W. Cai, Z.-L. Li, and Y. L. Ding, "In situ test study of characteristics of coal mining dynamic load," *Shock and Vibration*, vol. 2015, Article ID 121053, 8 pages, 2015.

[30] D.-D. Jiang, "*Experimental study on the relationship between microstructal characteristic and fragment size of rock under dynamic loading*," M.S. thesis, University of Science and Technology Liaoning, Anshan, China, 2016.

[31] J.-M. Xu, J.-C. Gu, A.-M. Chen, X.-Y. Zhang, and Z.-Q. Ming, "Study of anti-explosion ability of reinforced tunnels with different anchor lengths and spacings," *Rock and Soil Mechanics*, vol. 33, no. 11, pp. 3489–3496, 2012.

[32] S. Shah and E. Hoek, "Simplex reflection analysis of laboratory strength data," *Canadian Geotechnical Journal*, vol. 29, no. 2, pp. 278–287, 1992.

[33] C. Srinivasan, S.-K. Arora, and R.-K. Yaji, "Use of mining and seismological parameters as premonitors of rockbursts," *International Journal of Rock Mechanics and Mining Science & Geomechanics Abstracts*, vol. 34, no. 6, pp. 1001–1008, 1997.

[34] G.-F. Wang, S.-Y. Gong, Z.-L. Li, L.-M. Dou, W. Cai, and Y. Mao, "Evolution of stress concentration and energy release before rock bursts: two case studies from Xingan Coal Mine, Hegang, China," *Rock Mechanics and Rock Engineering*, vol. 49, no. 8, pp. 3393–3401, 2016.

[35] G.-F. Wang, S.-Y. Gong, L.-M. Dou, W. Cai, X.-Y. Yuan, and C.-J. Fan, "Rockburst mechanism and control in coal seam with both syncline and hard strata," *Safety Science*, vol. 115, pp. 320–328, 2019.

[36] E. Hoek, P.-K. Kaiser, and W.-F. Bawden, *Support of Underground Excavations in Hard Rock*, A.A. Balkema, Rotterdam, Netherlands, 1995.